OPTICAL REVIEW Vol. 20, No. 5 (2013) 438–441

The Early-Stage Diagnosis of Albinic Embryos by Applying Optical Coherence Tomography

Bor-Wen YANG*, Shih-Yuan WANG, Yu-Yen WANG, Jyun-Jhang CAI, and Chung-Hao CHANG

Department of Opto-Electronic System Engineering, Minghsin University of Science and Technology, Hsinchu, Taiwan 30401, R.O.C.

(Received February 13, 2013; revised June 9, 2013; Accepted June 27, 2013)

Albinism is a kind of congenital disease of abnormal metabolism. *Poecilia reticulata* (guppy fish) is chosen as the model to study the development of albinic embryos as it is albinic, ovoviviparous and with short life period. This study proposed an imaging method for penetrative embryo investigation using optical coherence tomography. By imaging through guppy mother's reproduction purse, we found the embryo's eyes were the early-developed albinism features. As human's ocular albinism typically appear at about four weeks old, it is the time to determine if an embryo will grow into an albino.

Keywords: albinism, Poecilia reticulata, optical coherence tomography, ocular albinism

1. Introduction

Albinism is a recessive defect in melanin metabolism in which pigment is absent from hair, skin and eyes (oculocutaneous albinism) or from the eyes only (ocular albinism).[1,2] These patients are in lack of threonine, an enzyme helping phenol to be oxidized as melanin; that is, melanin is an end product of the metabolism mechanism of amino acid tyrosine. When the skin of albinos is exposed to sunlight, it gradually darkens due to gradual increase in melanin. As albinism has no effective therapy, it becomes important in its early-time diagnosis. In today's technology, the pickup of embryo's cells throuth a human mother's womb can derive the baby's gene atlas and judge some of its inherited abnormalities, while the expense is beyond average people's affordability. To decrease the albinism birthrate and to solve related social problems, we proposed a medical imaging scheme to examine the embryo through its mother's belly and to judge whether it will become an albino.

2. Materials and Methods

By principle of developmental biology, the albinic individuals between vertebrate species have great similarity in morphology.[1)] To study the albinism features of vertebrates' embryos, we choose *Poecilia reticulata* (guppies, or peacock fishes) as the samples because: (1) they have both normal and albinic varieties, as shown in Fig. 1; (2) they are ovoviviparous, similar to viviparous vertebrates in the reproduction way; (3) they have short lifetime, typically only four weaks; (4) compared to other species, it is easier to observe the guppy embryos through their mothers' reproduction purses. All modern medical imaging technologies have their own advantages and limitations. Due to non-invasiveness and spatial resolution as high as 1–10 μm, optical coherence tomography (OCT) was extensively applied in ophthalmology, dermatology and gastroenterology.[3)] Most studies on oculocutaneous albinism by OCT were dedicated to the inspection of abnormal morphology of foveal hypoplasia;[4–6)] however, we aimed albinism imaging by OCT at early-stage diagnosis so that the results can be applied to solve social problems.

(a) (b)

Fig. 1. (Color online) (a) The normal peacock fish and (b) the albinic peacock fish.

Our first challenge was to find the growing eyes of normal and albinic guppy embryos, which were typically as tiny as ~200 μm; the other one was to do this penetratively through their mothers' reproduction purses. To examine the developing details of guppy embryos, we could adopt RGB LED as source to implement a full-color OCT system with 10-μm resolution.[7)] Compared with narrow bandwidth of lasers and LD, RGB LED was suitable for low-coherence imaging applications. Besides, RGB LED has merits of small volume, long lifetime, and easy to be integrated as a tri-color source module. As shown in Figs. 2(a) and 2(b), the central portion of the OCT system shows a 2×2 optical coupler, which acts as the interferometry core. The top right denotes the RGB LED sources and the related optics. The bottom right shows the sample arm to scan the guppy during inspection process. This arm consists of a fiber lens for collimation and an objective lens to focus the scanning beam. The interference signal is received by a high-speed optical detector and then fed to a personal computer for image processing. The R, G, and B images from identical tissue cross-section were derived by a floating objective lens, which is a 20× microscope objective lens controlled by a

*E-mail address: bwyang@must.edu.tw

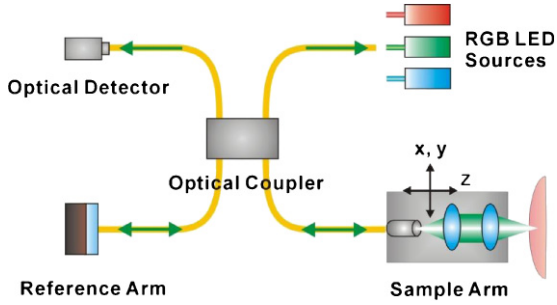

(a)

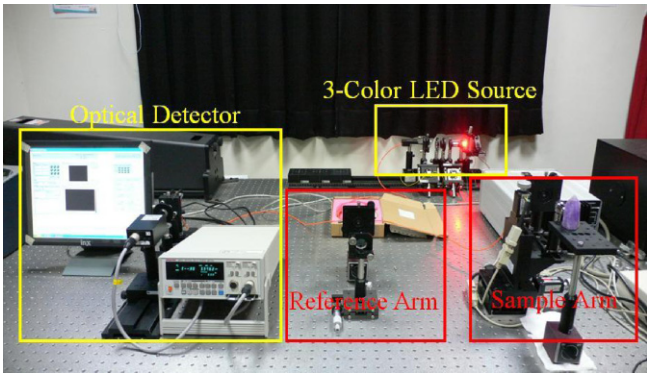

(b)

Fig. 2. (Color online) The OCT system for non-invasive inspection of guppy's reproduction purse.

10 nm-resolution motoring engine. The motorizing engine is made of a three-dimensional program-controlled stepper, on which the fiber end to detect the sample, the GRIN lens to collimate the beam, and the microscope objective for focusing are equipped, as depicted in Fig. 2. Overlapping the R, G, and B images will produce a full-color image of the sample tissue.

When we light the red LED in Fig. 2, the OCT system detects the red light back-scattered from the scanned point of the tissue to interfere with the red beam reflected from the reference arm. The intensity of this red interference signal is proportional to that of the red light scattered from the scanned point, which is exactly the red content the sampled point contains. As shown in Fig. 3(a), our system employed self-developed LabVIEW™ program to transform the time-resolved interference signal (top right block) into a real-time red image (bottom right block), and finally into a complete R, G, or B image (bottom left block). The top left block indicated the panel used to control the scanning activities of sample arm. Due to the dispersion of R, G, B focal planes, a floating objective lens was equipped into the OCT system to achieve the confocal requirement. A full-color tomography of sample tissue could be derived by overlapping three confocal R, G, and B single-color images. Figure 3(b) illustrated the program interface to superimpose the R, G, and B images (shown in the middle row) to form a full-color image (top right block), which showed the micro-capillary system of a guppy mother's reproduction purse.

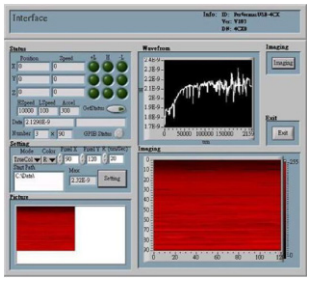

(a)

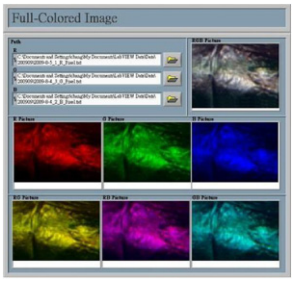

(b)

Fig. 3. (Color online) (a) A LabVIEW™ program developed to transform the interference signal stream into an R, G or B image; (b) The program interface used to overlap three confocal R, G, and B images to derive a full-color sample image.

Table 1. The penetration depth (X), lateral (Y), and axial (Z) resolutions of the R, G, and B beams, where the peak wavelengths (λ_p) and FWHMs ($\Delta\lambda$) are as follows: red: $\lambda_p = 640$ nm, $\Delta\lambda = 15$ nm; green: $\lambda_p = 525$ nm, $\Delta\lambda = 30$ nm; blue: $\lambda_p = 450$ nm, $\Delta\lambda = 19$ nm.

	X (mm)	Y (μm)	Z (μm)
Red LED	0.758	0.679	12.05
Green LED	0.686	0.557	4.054
Blue LED	0.636	0.477	4.703

3. Results and Discussion

3.1 Penetration depth and resolutions

The penetration depth, lateral, and axial resolutions of the source rays are derived by $1/(\pi f \mu_0 \sigma)^{1/2}$, $2\lambda_p/(\pi \mathrm{NA})$, and $2(\ln 2) \cdot \lambda_p{}^2/(\pi \Delta\lambda)$, respectively,[7] as summarized in Table 1. Driven by a current of ~1.35 A, each of the LEDs delivers a flux of ~350 lm.[8] Note that the image of guppy's micro-capillary system contains all three R, G, and B components because the imaging depth in Fig. 3(b) was smaller than 0.636 mm. As the R, G, and B sample beams are focused onto different imaging planes due to dispersion, the objective lens should be shifted towards or away from the sample surface to achieve confocal requirement for ideal image superimposition. As shown in Fig. 4, for a distance A shifting between the objective and the sample surface, the focusing depths B_1, B_2, and B_3 of the B, G, and R beams were derived through TracePro™ modeling.[9] The simulation results are summarized in Table 2.

3.2 Non-invasive OCT images

By en-face scanning scheme, the eye images of a 2-week-old normal embryo and a two-week-old albinic embryo were obtained through their mothers' reproduction purses respectively, as shown in Figs. 5(a) and 5(b). We adjusted the position of the objective lens by the motorizing engine so that the distance (A) between the lens and the guppy's purse became 0.72 mm. Referring to the data listed in Table 2, the focusing depth (B_3) of the red beam would be 0.7190 mm accordingly. Since the focusing depth of 0.7190 mm was

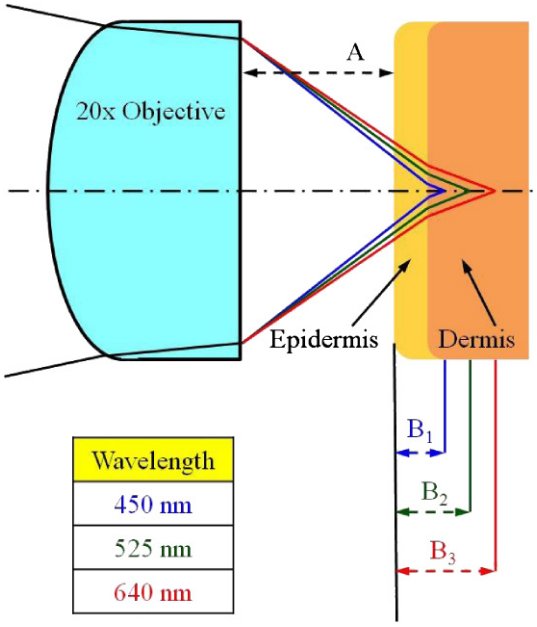

Fig. 4. (Color online) TracePro™ modeling to derive the focusing depths of B, G, and R beams incident to a sample skin. The 20× objective has a numerical aperture of 0.40 and a focal length of 6.9 mm.

Table 2. Dependence of the focusing depths of B, G, and R rays (B_1, B_2, and B_3) on the distance between the objective lens and sample surface (A).

A (mm)	B_1 (mm)	B_2 (mm)	B_3 (mm)
0.70	0.5616	0.6557	0.7462
0.72	0.5333	0.6259	0.7190
0.75	0.4906	0.5847	0.6762
0.79	0.4386	0.5327	0.6242
0.80	0.4197	0.5144	0.6055
0.85	0.3488	0.4430	0.5363
0.90	0.2790	0.3739	0.4627

beyond the penetration depth of G and B beams (0.686 and 0.636 mm, respectively, by Table 1), only the R-component image was found in the overlapped image eventually, as revealed in Figs. 5(a) and 5(b). It was found that the eye of the albinic embryo (b) was apparently lighter than that of the normal one (a). Both images consisted of 160 × 120 pixels, each with $10 \times 10\,\mu m^2$ pixel size. The eyeballs of the embryos were estimated as ~200 μm in size. From Figs. 5(a) and 5(b), we could distinguish between the normal and albinic embryos at their age of only two weeks old completely non-invasively just from their eye images through their mothers' purses.

To confirm the OCT images displayed in Figs. 5(a) and 5(b) were truly derived from the embryo eyes, we dissected the two guppy mothers' purses after OCT imaging and took out the two embryos for further inspection. The digital camera (DC) pictures of the two 2-week-old embryos were shown in Figs. 6(a) and 6(b). We found the eyes of the

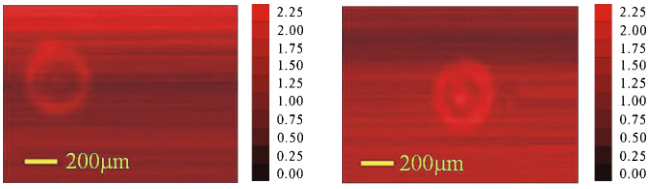

(a) (b)

Fig. 5. (Color online) The eye images of (a) a normal and (b) an albinic guppy embryo obtained through their mothers' reproduction purses by the OCT imaging system (scale bar: 200 μm; the unit used in the intensity bar is 10^{-9} mW).

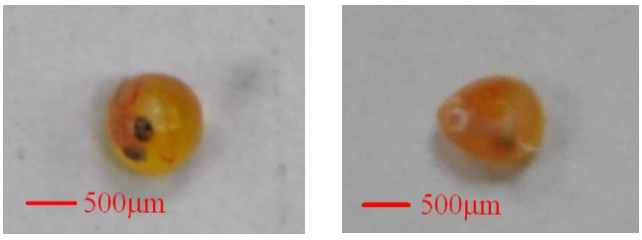

(a) (b)

Fig. 6. (Color online) The DC pictures of (a) a normal and (b) an albinic guppy embryo taken from their mothers' urses at the age of two weeks old (scale bar: 500 μm).

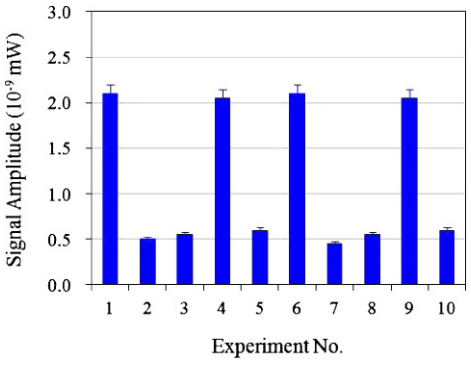

(a)

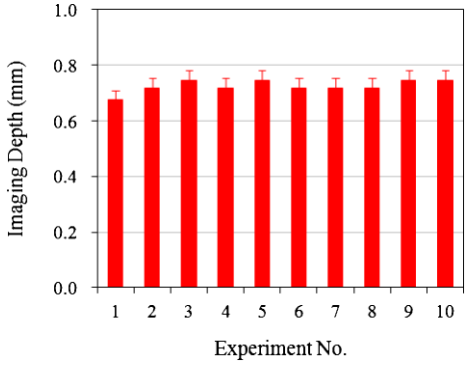

(b)

Fig. 7. (Color online) The imaging results of ten guppy embryos through their mothers' reproduction purses by the OCT system: (a) the signal amplitudes of the embryo eye; (b) the imaging depths of the embryo eye, respectively.

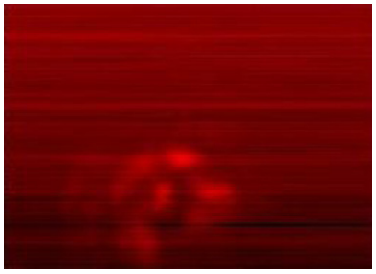

(a)

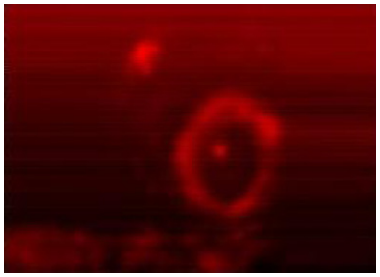

(b)

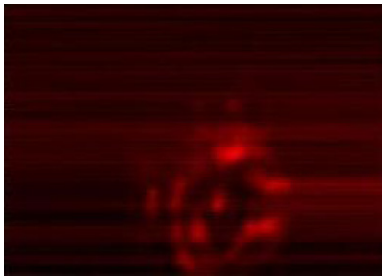

(c)

Fig. 8. (Color online) Three of albinic eyeball images obtained from imaging depth of (a) 0.676, (b) 0.719, and (c) 0.746 mm, respectively.

normal and albinic embryos were really dark and bright, respectively, just the same as the images shown in Figs. 5(a) and 5(b). In the future, the embryos presented in Figs. 6(a) or 6(b) will grow to be a normal (with dark eyes) or an albinic (with light eyes) guppy fish, respectively, as shown in Figs. 1(a) and 1(b). Ten similar imaging experiments were performed, where the signal amplitudes and imaging depths of the sampled embryo eyes were summarized in Figs. 7(a) and 7(b), respectively. From Fig. 7(a), we confirmed that the ten sampled guppy embryos growed later to be six normal and four albinic babies, respectively. By Fig. 7(b), we found 4 of the embyos were sampled at the depth of 0.746 mm, 5 of them were imaged at the depth of 0.719 mm, and only 1 of them was detected at the focal depth of 0.676 mm. Three of albinic eye images obtained from different focusing depths 0.676 mm (Sample No. 1 in Fig. 7), 0.719 mm (Sample No. 4 in Fig. 7), and 0.746 mm (Sample No. 9 in Fig. 7) are presented in Figs. 8(a) to 8(c) for further confirmation, respectively. By Figs. 6(a) and 6(b), the size of guppy embryoes are found about 0.7–0.9 mm in length, which implies the embryo eyes distributed in the deeper region are beyond the limitation of penetration depth of the red beam in the OCT system.

4. Conclusion

Without sufficient melanin, the albinos suffer from whitened hair and skin, sensitivity to light, and difficulty in social accommodation.[10] As it is still expensive and challenging to obtain genes to confirm albinism by womb puncture, the embryo inspection through mother's belly by medical imaging method provides a feasible solution. The eye is one of the early-developed organs in vertebrate animals, and one of the albinic features in certain animals. By non-invasive detection on normal and albinic embryos, it was found the eyeballs were the first-examined albinism features.

Acknowledgment

This work is supported by National Science Council of Taiwan under Contract No. NSC 102-2622-E-159-001-CC1.

References

1) J. Gerhart and M. Kirschner: *Embryos and Evolution* (Blackwell, New York, 1997).
2) P. J. Bowler: J. Hist. Ideas **36** (1975) 95.
3) D. Huang, E. A. Swanson, C. P. Lin, J. S. Schuman, W. G. Stinson, W. Chang, M. R. Hee, T. Flotte, K. Gregory, C. A. Puliafito, and J. G. Fujimoto: Science **254** (1991) 1178.
4) C. H. Meyer, D. J. Lapolice, and S. F. Freedman: Am. J. Ophthalmol. **133** (2002) 409.
5) J. H. Seo, Y. S. Yu, J. H. Kim, H. K. Choung, J. W. Heo, and S.-J. Kim: Ophthalmology **114** (2007) 1547.
6) G. T. Chong, S. Farsiu, S. F. Freedman, N. Sarin, A. F. Koreishi, J. A. Izatt, and C. A. Toth: Arch. Ophthalmol. **127** (2009) 37.
7) B.-W. Yang, L.-M. Chan, and K.-C. Wang: Opt. Rev. **16** (2009) 392.
8) Edison Opto Corporation, Taipei, Taiwan [http://www.edison-opto.com.tw/].
9) T. H. Shao: *Engineering Optics: Optical Design* (Electronic Industry Press, Beijing, 2003).
10) G. Baikoff, E. Lutun, J. Wei, and C. Ferraz: *An in vivo OCT Study of Human Natural Accommodation in a 19-Year-Old Albin* (Clinique Monticelli, Marseille, 2005).